

Phenylbenzimidazole-Based New Bipolar Host Materials for Efficient Phosphorescent Organic Light-Emitting Diodes

Shin-ya Takizawa, Victor A. Montes, and Pavel Anzenbacher, Jr.*

Department of Chemistry and Center for Photochemical Sciences, Bowling Green State University,
Bowling Green, Ohio 43403

Received February 18, 2009. Revised Manuscript Received April 20, 2009

Two new bipolar host materials based on a 1,3,5-tris(*N*-phenylbenzimidazol-2-yl)benzene (TPBI) core with the carbazole and diphenylamine groups were designed, synthesized, and applied in phosphorescent organic light-emitting diodes (PhOLEDs). The DFT calculations indicated desirable distribution of HOMO and LUMO densities, suggesting potential for bipolar charge transport. In addition, the electrochemical and phosphorescence studies revealed that neither the LUMO level nor the triplet energies differ significantly from the parent TPBI suggesting that the new materials would be suitable as hosts capable of both electron and hole transport and suitable for harvesting green electrophosphorescence. As a result of broader charge recombination zone resulting from the bipolar properties of new hosts, the devices with a simple architecture achieved significantly better current efficiencies of 48 and 60 cd/A (the power efficiencies of 46 and 70 lm/W), compared with a device using conventional TPBI host (19 cd/A; 21 lm/W) as well as a more complex device utilizing 4,4',4''-tris(*N*-carbazolyl)triphenylamine (TCTA) as an exciton blocking layer.

Introduction

In the last decade, efforts have been devoted to the development of materials useful for the fabrication of organic light-emitting diodes (OLEDs).^{1,2} The OLED performance was found to depend not only on the luminescence efficiency of the emissive materials but equally importantly also on the optical and semiconductor characteristics of hosts and charge-transporting materials.² Because of the multiplicity of factors influencing these features, molecular design of such materials is fairly complicated as it requires optimizing properties that include HOMO–LUMO levels, triplet excited states energy levels, film forming behavior, thermal stability, and suitable emission wavelength. Here, phosphorescent OLEDs (PhOLEDs) employing phosphorescent emitters doped into a proper charge transporting host material have attracted significant attention because of their high efficiencies as a consequence of the utilization of both singlet and triplet excitons.^{1d} A number of approaches to realize highly efficient PhOLEDs were adopted focusing on limiting triplet–triplet annihilation,^{3–5} triplet–polaron quenching due to triplet energy transfer to charged molecules,⁵ or exciton dissociation at high current density or luminance.⁶ These triplet quenching processes may be correlated with materials

employed and device architectures used. In particular, the PhOLEDs utilizing phosphors with long triplet excited state lifetime and a narrow charge recombination zone are prone to triplet–triplet exciton quenching due to a local high density of triplet excitons.⁵ This problem is further exacerbated by the relatively long diffusion of the triplet excitons.⁷

Thus, materials with balanced charge transport that can generate broad charge recombination zones are widely sought. However, with few exceptions,⁸ most semiconductor host materials transport holes⁹ or electrons.¹⁰ In fact, most electron transporters also display hole-blocking properties, and most hole transporters display electron-blocking capacity. Thus, in general, in a device utilizing a hole-transporting host, the recombination zone is likely to be located close to the host–electron transport layer (ETL) interface. Similarly,

- (3) Kepler, R. G.; Caris, J. C.; Avakian, P.; Abramson, E. *Phys. Rev. Lett.* **1963**, *10*, 400.
 (4) Ern, V.; Bouchriha, H.; Fourny, J.; Delacote, G. *Solid State Commun.* **1971**, *9*, 1201.
 (5) (a) Baldo, M. A.; Adachi, C.; Forrest, S. R. *Phys. Rev. B* **2000**, *62*, 10967. (b) Reineke, S.; Walzer, K.; Leo, K. *Phys. Rev. B* **2007**, *75*, 125328. (c) Reineke, S.; Schwartz, G.; Walzer, K.; Leo, K. *Appl. Phys. Lett.* **2007**, *91*, 123508.
 (6) Kalinowski, J.; Stampor, W.; Mezyk, J.; Cocchi, M.; Virgili, D.; Fattori, V.; Di Marco, P. *Phys. Rev. B* **2002**, *66*, 235321.
 (7) Baldo, M. A.; O'Brien, D. F.; Thompson, M. E.; Forrest, S. R. *Phys. Rev. B* **1999**, *60*, 14422.
 (8) (a) Hancock, J. M.; Gifford, A. P.; Zhu, Y.; Lou, Y.; Jenekhe, S. A. *Chem. Mater.* **2006**, *18*, 4924. (b) Liao, Y.-L.; Lin, C.-Y.; Wong, K.-T.; Hou, T.-H.; Hung, W.-Y. *Org. Lett.* **2007**, *9*, 4511. (c) Lai, M.-Y.; Chen, C.-H.; Huang, W.-S.; Lin, J. T.; Ke, T.-H.; Chen, L.-Y.; Tsai, M.-H.; Wu, C.-C. *Angew. Chem., Int. Ed.* **2008**, *47*, 581. (d) Su, S.-J.; Sasabe, H.; Takeda, T.; Kido, J. *Chem. Mater.* **2008**, *20*, 1691. (e) Su, S.-J.; Gonmori, E.; Sasabe, H.; Kido, J. *Adv. Mater.* **2008**, *20*, 4189. (f) Ge, Z.; Hayakawa, T.; Ando, S.; Ueda, M.; Akiike, T.; Miyamoto, H.; Kajita, T.; Kakimoto, M. *Adv. Funct. Mater.* **2008**, *18*, 584. (g) Son, K. S.; Yahiro, M.; Imai, T.; Yoshizaki, H.; Adachi, C. *Chem. Mater.* **2008**, *20*, 4439. (h) Gao, Z. Q.; Luo, M.; Sun, X. H.; Tam, H. L.; Wong, M. S.; Mi, B. X.; Xia, P. F.; Cheah, K. W.; Chen, C. H. *Adv. Mater.* **2009**, *21*, 688.

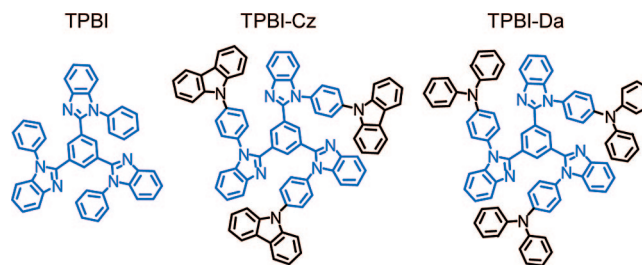
* Corresponding author. E-mail: pavel@bgsu.edu.

- (1) (a) Shinar, J., Ed. *Organic Light-Emitting Devices, A Survey*; AIP Press/Springer: New York, 2003. (b) Kafafi, Z. H., Ed. *Organic Electroluminescence*; CRC Press: Boca Raton, 2005. (c) Li, Z.; Meng, H., Eds. *Organic Light-Emitting Materials and Devices*; CRC Press: Boca Raton, FL, 2007. (d) Yersin, H., Ed. *Highly Efficient OLEDs with Phosphorescent Materials*; Wiley-VCH: Weinheim, Germany, 2008.
 (2) (a) Mitschke, U.; Bauerle, P. *J. Mater. Chem.* **2000**, *10*, 1471. (b) Kulkarni, A. P.; Tonzola, C. J.; Babel, A.; Jenekhe, S. A. *Chem. Mater.* **2004**, *16*, 4556. (c) Holder, E.; Langeveld, B. M. W.; Schubert, U. S. *Adv. Mater.* **2005**, *17*, 1109. (d) Shirota, Y.; Kagayama, H. *Chem. Rev.* **2007**, *107*, 953.

in the devices utilizing an electron transporting host the recombination zone would be located close to the hole-transporting layer (HTL).¹¹ This results in the narrow recombination zones formed in regions with a high polaron density. For this reason, materials capable of efficient transport of both holes and electrons should be able to generate broader recombination zones and steer them away from the interface with the charge-transport layers.¹² Such bipolar and ambipolar host materials are, however, still relatively rare⁸ and frequently do not yield the highest-efficiency devices. On the other hand, the lack of such materials can be compensated for by judicious use of exciton-blocking layers (EBL), which increases the efficiency but also the complexity and potential cost of the device.

To achieve highly efficient OLEDs, numerous classes of charge transporting materials have been reported. For example, the hole-transporting materials comprise triarylamine or carbazole moieties.¹³ On the other hand, the electron-transporting materials are structurally more diverse. Typical examples of them are tris(8-hydroxyquinolino)aluminum(III) (Alq₃),¹⁴ oxadiazole and triazole derivatives, and other nitrogen-containing electro-deficient materials.¹⁵ Owing to its large HOMO–LUMO energy gap, 1,3,5-tris(*N*-phenylbenzimidazol-2-yl)benzene (TPBI) has been recognized as a useful electron-transporter and as a host material for fluorescent and phosphorescent dopants.¹⁶ However, detailed investigation and optimization of the TPBI derivatives has not been reported so far. Such studies could further improve utility of TPBI and its derivatives in OLEDs, while the development of TPBI-based ambipolar transport materials and hosts could allow for substantial device architecture simplification and attendant cost reduction.⁸ As a result of a broad charge recombination zone in an emitting layer, such materials would have the potential for achieving a high

Chart 1. Structure of the Compounds in This Work



efficiency at low cost, thus being suitable for large area devices required, for example, for solid-state lighting.

In this study, we present two bipolar transporter–host materials, TPBI-Cz and TPBI-Da (Chart 1), based on the electron-transporting TPBI core with a large HOMO–LUMO gap functionalized with hole-transporting moieties, carbazole or diphenylamine. We report on their electronic and photonic properties and the characteristics of the corresponding PhOLEDs. While the TPBI core is known to transport electrons and display high triplet energy, the carbazole^{8d,9,17} and diphenylamine moieties¹³ are known to impart high hole mobility, and both have been widely used in hole-transporting materials.

Results and Discussion

Theoretical Calculation. Density functional theory (DFT) calculations (B3LYP; 6-31G*) were carried out to obtain information about the HOMO and LUMO distributions of the compounds. Figure 1 depicts the resulting HOMO and LUMO of the compounds. The theoretical model indicated a significant dihedral angle (64–67°) between the *N*-phenyl ring and the benzimidazole plane in all compounds. Figure 1 shows that neither HOMO nor LUMO is localized on the *N*-phenyl ring in TPBI, suggesting that introducing the carbazolyl or diphenylamino group on the *N*-phenyl ring would not result in a significant change in the LUMO levels of the TPBI core, which would then retain proper electron-transporting properties. On the other hand, the HOMO is expected to lie on the electron-rich groups, affording an effective hole-transporting property. In fact, DFT studies of TPBI-Cz and TPBI-Da clearly indicated that their LUMOs remain on the benzene core and benzimidazole moiety with similar distributions to that of TPBI, whereas the HOMOs are localized only on the carbazole or triphenylamine part (Figure 1).

Synthesis. TPBI was prepared following the modified literature method.¹⁸ As shown in Scheme 1, TPBI-Cz and TPBI-Da were successfully synthesized via TPBI tribromoderivative (TPBI-Br₃) by using Ullmann type and palladium catalyzed reactions, respectively. TPBI-Br₃ was synthesized as follows. The reaction of 1-fluoro-2-nitrobenzene and 4-bromoaniline in the presence of potassium fluoride gave *N*-(4-bromophenyl)-*N'*-(2-nitrophenyl)amine in 60% yield, followed by reduction of the nitro group with stannous chloride dihydrate (80%). The resulting diamine derivative

- (9) (a) Ikai, M.; Tokito, S.; Sakamoto, Y.; Suzuki, T.; Taga, Y. *Appl. Phys. Lett.* **2001**, *79*, 156. (b) Brunner, K.; Dijken, A.; Borner, H.; Bastiaansen, J. J. A.; Kiggen, N. M. M.; Langeveld, B. M. W. *J. Am. Chem. Soc.* **2004**, *126*, 6035. (c) Tsai, M.-H.; Lin, H.-W.; Su, H.-C.; Ke, T.-H.; Wu, C.-c.; Fang, F.-C.; Liao, Y.-L.; Wong, K.-T.; Wu, C.-I. *Adv. Mater.* **2006**, *18*, 1216. (d) Tsai, M.-H.; Hong, Y.-H.; Chang, C.-H.; Su, H.-C.; Wu, C.-C.; Matoliukstyte, A.; Simokaitiene, J.; Grigalevicius, S.; Grazulevicius, J. V.; Hsu, C.-P. *Adv. Mater.* **2007**, *19*, 862.
- (10) Adachi, C.; Baldo, M. A.; Forrest, S. R.; Thompson, M. E. *Appl. Phys. Lett.* **2000**, *77*, 904.
- (11) Adachi, C.; Baldo, M. A.; Thompson, M. E.; Forrest, S. R. *J. Appl. Phys.* **2001**, *90*, 5048.
- (12) Kim, S. H.; Jang, J.; Yook, K. S.; Lee, J. Y. *Appl. Phys. Lett.* **2008**, *92*, 023513.
- (13) Shirota, Y. *J. Mater. Chem.* **2000**, *10*, 1.
- (14) (a) Tang, C. W.; VanSlyke, S. A. *Appl. Phys. Lett.* **1987**, *51*, 913. (b) Montes, V. A.; Pohl, R.; Shinar, J.; Anzenbacher, P., Jr. *Chem.–Eur. J.* **2006**, *12*, 4523.
- (15) (a) Hughes, G.; Bryce, M. R. *J. Mater. Chem.* **2005**, *15*, 94. (b) Kim, J. H.; Yoon, D. Y.; Kim, J. W.; Kim, J.-J. *Synth. Met.* **2007**, *157*, 743.
- (16) (a) Gao, Z.; Lee, C. S.; Bello, I.; Lee, S. T.; Chen, R.-M.; Luh, T.-Y.; Shi, J.; Tang, C. W. *Appl. Phys. Lett.* **1999**, *74*, 865. (b) Adachi, C.; Baldo, M. A.; Forrest, S. R.; Lamansky, S.; Thompson, M. E.; Kwong, R. C. *Appl. Phys. Lett.* **2001**, *78*, 1622. (c) Ko, C.-W.; Tao, Y.-T.; Lin, J. T.; Thomas, K. R. *J. Chem. Mater.* **2002**, *14*, 353. (d) Duan, J.-P.; Sun, P.-P.; Cheng, C.-H. *Adv. Mater.* **2003**, *15*, 224. (e) Meyer, J.; Hamwi, S.; Bulow, T.; Johannes, H.-H.; Riedl, T.; Kowalsky, W. *Appl. Phys. Lett.* **2007**, *91*, 113506-1. (f) Kim, S. H.; Jang, J.; Lee, J. Y. *Appl. Phys. Lett.* **2008**, *91*, 083511. (g) Kondakova, M. E.; Pawlik, T. D.; Young, R. H.; Giesen, D. J.; Kondakov, D. Y.; Brown, C. T.; Deaton, J. C.; Lenhard, J. R.; Klubek, K. P. *J. Appl. Phys.* **2008**, *104*, 094501.

(17) Agata, Y.; Shimizu, H.; Kido, J. *Chem. Lett.* **2007**, *36*, 316.

(18) Shi, J.; Tang, C. W.; Chen, C. T. U.S. Patent No. 5,646,948, 1997.

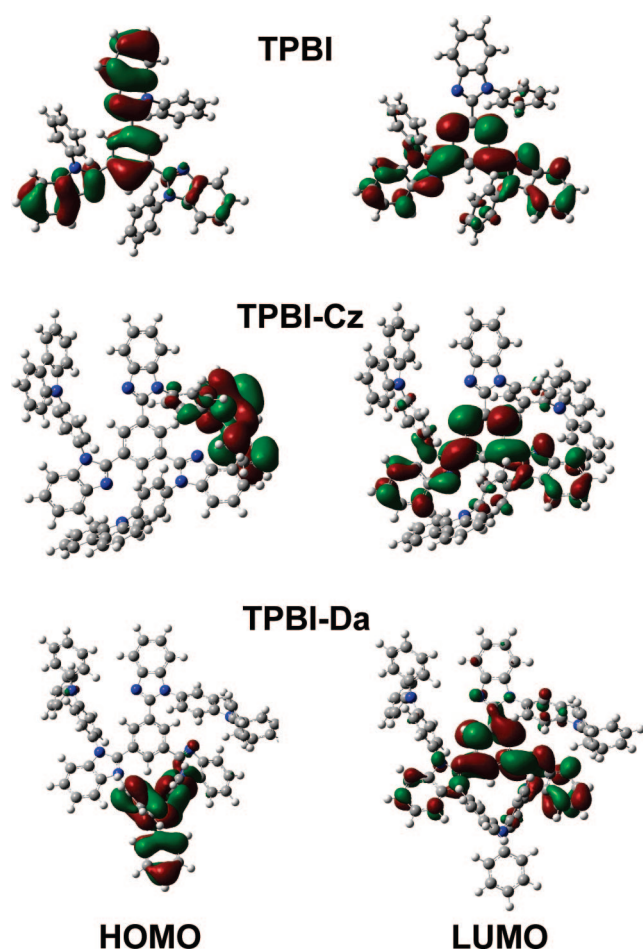
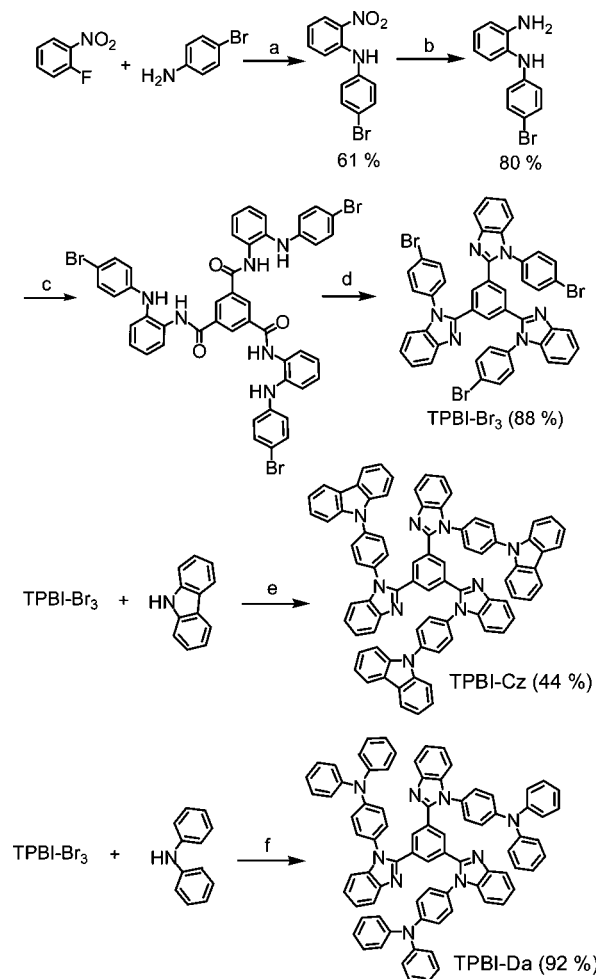


Figure 1. HOMO and LUMO distributions obtained from DFT calculations of TPBI, TPBI-Cz, and TPBI-Da.

136 reacted with 1,3,5-benzenetricarbonyl trichloride to produce
 137 the corresponding triamide, which was then used without
 138 purification in the next condensation reaction. Finally, TPBI-
 139 Br₃ was prepared from the trisbenzamide in 88% yield by
 140 heating at 250 °C. It should be noted that TPBI-Br₃ is a useful
 141 intermediate for introduction of many different structural
 142 features by using various coupling reactions, which are
 143 currently being explored in our laboratory.

144 **Electrochemical Properties.** Cyclic voltammetry (CV)
 145 was performed to investigate the redox behavior of the
 146 compounds. However, no clear reduction wave was observed
 147 in the potential window of the cyclic voltammograms. With
 148 respect to oxidation, only TPBI-Da underwent a reversible
 149 oxidation process while TPBI and TPBI-Cz exhibited ir-
 150 reversible oxidation waves. To determine the HOMO and
 151 LUMO energy levels in TPBI-Cz and TPBI-Da, the redox
 152 potentials were estimated using differential pulse voltam-
 153 metry (DPV) (Table 1).¹⁹ From the DPV data, the carbazolyl
 154 and diphenylamino groups on the *N*-phenyl ring were found
 155 to have a major effect especially on the HOMO level of
 156 TPBI. For instance, these groups negatively shifted the
 157 oxidation potential of TPBI by 0.31 and 0.63 V, respectively.
 158 On the other hand, the reduction potentials of TPBI-Cz and
 159 TPBI-Da proved to be almost identical to that of TPBI. It
 160 is noteworthy that these results are consistent with the predic-
 161 tions from DFT calculations, which had shown that the

Scheme 1. Synthesis of TPBI-Br₃, TPBI-Cz, and TPBI-Da^a



^a Conditions: (a) KF, 170–180 °C, 72 h; (b) SnCl₂·2H₂O, EtOH, reflux, 24 h; (c) 1,3,5-benzenetricarbonyl trichloride, NMP, r.t. to 50 °C, 2.5 h; (d) 250 °C, 3 h; (e) CuI, 18-crown-6, K₂CO₃, DMPU, 210 °C, 64 h; (f) Pd(OAc)₂, P(*t*-Bu)₃, NaO^tBu, toluene, 110 °C, 70 h.

LUMO energy level of TPBI-Da and TPBI-Cz remained
 close to that of TPBI and that all compounds had identical
 LUMO distributions as seen in Figure 1. In TPBI-Da, com-
 pared with TPBI-Cz, a decreased HOMO–LUMO gap was
 observed due to the increased HOMO level in TPBI-Da. This
 is presumably due to the stronger electron-donating effect
 of the diphenylamino group compared to that of carbazole.

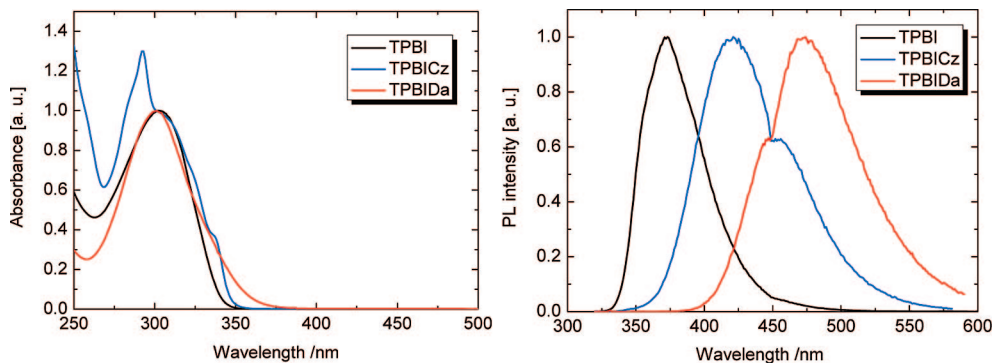
Spectroscopic Studies. Table 1 summarizes photophysical
 data of TPBI, TPBI-Cz, and TPBI-Da. The UV–vis and PL
 spectra at room temperature were recorded in dichloro-
 methane solutions (see Figure 2). The UV–vis absorption
 spectra of TPBI, TPBI-Cz, and TPBI-Da exhibited nearly
 identical absorptions at 292–303 nm attributable to the
 π – π^* transition. However, the end absorption of TPBI-Da
 was red-shifted by approximately 40 nm. Interestingly, TPBI-
 Cz showed both the peak at 292 nm as well as a shoulder at
 300 nm. This observation suggests that the *N*-phenylcar-
 bazole moiety tilts against the benzimidazole plane and behaves

(19) In a recent paper, the HOMO and LUMO energy levels of TPBI have been reported to be –6.3 and –2.8 eV, respectively.^{16c} The difference from our data may come from different measurement methods or conditions (e.g., cyclic voltammetry, differential pulse voltammetry in solution, and ultraviolet photoelectron spectroscopy in the thin film).

Table 1. Photophysical and Electrochemical Properties and HOMO–LUMO Energy Levels of the Compounds

	$\lambda_{\text{max,abs}}$, nm (ϵ) ^a	λ_{em} (RT), nm ^a	λ_{em} (77 K), nm ^b	τ_{p} , ms ^c	E_{T} , eV	E^{ox} , V ^d	E^{red} , V ^d	HOMO, eV	LUMO, eV	HOMO–LUMO gap, eV
TPBI	303 (5.66×10^4)	373	465; 498; 536	20.6	2.67	1.23	−2.70	−6.03	−2.10	3.93
TPBI-Cz	292 (9.35×10^4)	421	465; 498; 534	65.9	2.67	0.92	−2.65	−5.72	−2.15	3.57
TPBI-Da	301 (1.22×10^5)	474	459; 489; 523	23.2	2.70	0.60	−2.73	−5.40	−2.07	3.33

^a In CH_2Cl_2 . ^b In 2-MeTHF glass. ^c Phosphorescence lifetime. ^d Determined by DPV of 1.0 mM solutions in CH_2Cl_2 containing tetrabutylammonium perchlorate and referenced against Fc/Fc^+ (0.360 V vs Ag/AgNO_3).

**Figure 2.** UV–vis absorption (left) and fluorescence spectra (right) of the compounds in CH_2Cl_2 solution.

180 as a fairly independent electronic entity. This is in accordance
181 with the fact that *N*-phenylcarbazole displays a strong
182 absorption at the same wavelength (292 nm).^{15b} It also
183 confirms the prediction that TPBI-Cz would not display
184 strong electronic coupling between *N*-phenylcarbazole and
185 the benzimidazole ring, thus affording the possibility of
186 separated hole and electron-transporting functions within the
187 molecule. This is further supported by the theoretical model
188 from DFT calculation for TPBI-Cz, which showed the
189 separated HOMO–LUMO distributions (Figure 1). The fluo-
190 rescence spectrum of TPBI shows an emission maximum at
191 373 nm, while the TPBI-Cz and TPBI-Da display red-shifted
192 maxima of 421 and 474 nm, respectively.

193 For host materials to yield highly efficient PhOLEDs, it
194 is also necessary that the triplet level of the host be higher
195 than that of the phosphorescent emitter. The high host triplet
196 levels are essential for a high efficiency as it prevents the
197 back energy transfer to hosts from phosphorescent dopants.²⁰
198 In the case of hosts with high triplet energy, the triplets tend
199 to form or be trapped on the phosphorescent dopant-emitter
200 and generate phosphorescence. The triplet energies of the
201 hosts are obtained directly from the time-gated phosphores-
202 cence spectra recorded at 77 K. On the basis of their long
203 lifetimes (Table 1), it was confirmed that all of the spectra
204 correspond to the triplet excited state. The phosphorescence
205 spectra exhibited three peaks, where TPBI showed phos-
206 phorescence 0–0 maximum at 465 nm corresponding to
207 triplet energy of 2.67 eV, while the TPBI-Cz and TPBI-Da
208 exhibited 0–0 transitions at 465 and 460 nm (2.67 eV, 2.70
209 eV). Thus, the triplet energies of TPBI-Cz and TPBI-Da are
210 equal or higher compared to TPBI. This further confirms
211 the hypothesis that the TPBI moiety is separated from the
212 carbazole and diphenylamine moieties suggested by the DFT
213 calculations. Another interesting finding is the fact that there
214 is no direct relationship between fluorescence spectral shift

and phosphorescence, that is, triplet level. This can be
explained by a remarkable difference in the exchange
energies, which were estimated from phosphorescence and
fluorescence at 77 K ($\Delta E_{\text{S-T}} = 0.88$ eV for TPBI, 0.67 eV
for TPBI-Cz, 0.38 eV for TPBI-Da). In the case of TPBI-
Da, the phosphorescence appears in almost the same spectral
region as fluorescence. The nature of the emissive state
corresponding to the luminescence processes has been
assigned to the respective singlet (τ_{f} 7.43 ns) and triplet (τ_{p}
23.2 ms) excited states using the luminescence lifetime
measurements. The data above suggest that, similarly to the
parent TPBI, TPBI-Cz and TPBI-Da would sufficiently
confine triplet energy of green phosphorescent dopants such
as iridium(III) bis(2-phenylpyridinato-*N,C'*)acetylacetonate
[$\text{Ir}(\text{ppy})_2(\text{acac})$] ($E_{\text{T}} = 2.30$ eV)¹¹ and would also act as a
bipolar host material for efficient green and red PhOLEDs
with simplified configuration.

Phosphorescent Organic Light-Emitting Diodes. To
demonstrate the ability of new TPBI-Cz and TPBI-Da host
materials to confine excitons corresponding to the dopants
with $E_{\text{T}} \leq 2.60$ eV and to test their ambipolar nature, we
fabricated green PhOLEDs using the following simple three-
layer configuration: indium tin oxide (ITO)/poly(ethylene-
dioxythiophene) doped with poly(styrenesulfonate) (PEDOT:
PSS) (30 nm) was used as a hole-injection layer, followed
by 4,4'-bis[*N*-(1-naphthyl)-*N*-phenylamino]biphenyl (α -NPD)
(40 nm) hole-transporting layer, which was then followed
by a blend of a host doped with 6% $\text{Ir}(\text{ppy})_2(\text{acac})$ to form
the emissive layer (50 nm). The devices were finalized by
deposition of CsF(1 nm)/Al(100 nm) cathode (Figure 3A).
A control device using TPBI as a host and electron transport
layer was also fabricated. To demonstrate the potential of
the TPBI-Cz/Da materials to yield efficient devices with
simpler architecture, a TPBI device with a 4,4',4''-tris(*N*-
carbazolyl)triphenylamine (TCTA) as an exciton-blocking
layer (EBL) was also fabricated (Figure 3B). Table 2
summarizes the electroluminescent data of the devices.

(20) Kawamura, Y.; Goushi, K.; Brooks, J.; Brown, J. J.; Sasabe, H.; Adachi, C. *Appl. Phys. Lett.* **2005**, *86*, 071104.

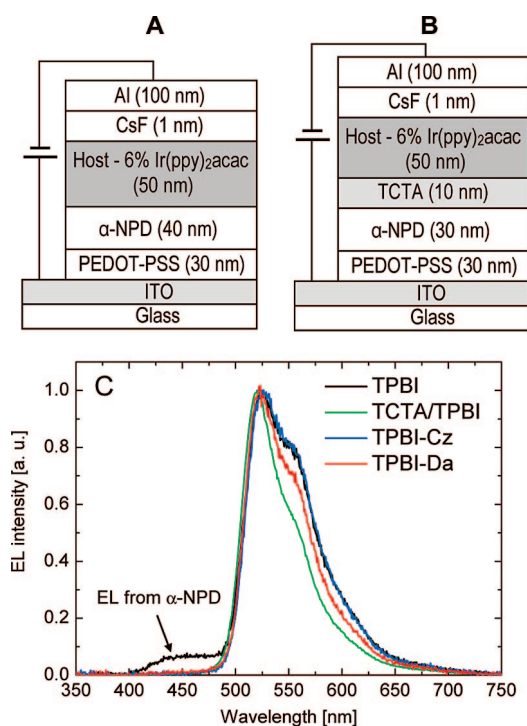


Figure 3. Panel A: Architecture of the three-layer PhOLED. Panel B: Analogous TCTA(EBL)-TPBI device. Panel C: EL spectra of the devices at 10 000 cd/m².

Table 2. Electroluminescence characteristics of the phosphorescent OLEDs

host	$\eta_{\text{ext.}}^a$ %	η_c^b cd A ⁻¹	η_p^c lm W ⁻¹	L_{max}^d cd m ⁻²	CIE ^e (x, y)
TPBI	4.7	18.8	21.0	63800	0.33, 0.58
TCTA-TPBI	5.7	26.4	33.2	78200	0.29, 0.64
TPBI-Cz	14.0	48.2	46.0	55500	0.34, 0.62
TPBI-Da	15.0	59.2	70.0	48400	0.32, 0.62

^a External quantum efficiency (EQE, %, at 0.1 mA/cm²). ^b Current efficiency at 0.1 mA/cm². ^c Power efficiency at 0.1 mA/cm². ^d Maximum luminance. ^e Commission Internationale de l'Éclairage coordinates at 10 000 cd/m².

252 The electroluminescence (EL) spectra recorded from
 253 devices, each comprising one of the four hosts (TPBI-only,
 254 TCTA-TPBI, TPBI-Cz, and TPBI-Da, Figure 3C), were
 255 examined. The TPBI-only device displayed α -NPD emission
 256 in the EL spectrum suggesting that the charge recombination
 257 occurs on the NPD-TPBI interface. This is likely due to
 258 low HOMO level and a low hole mobility in TPBI (see
 259 HOMO-LUMO energies in Figure 4). In the TPBI-only
 260 device we presume formation of a narrow exciton generation
 261 zone with high triplet exciton density, leading to the low
 262 EL efficiency (maximum power efficiency: 21 lm/W, current
 263 efficiency: 19 cd/A) as a result of triplet-polaron and
 264 triplet-triplet annihilation⁵ as well as triplet energy loss to
 265 the adjacent α -NPD layer ($E_T = 2.29$ eV).²¹ The incorpora-
 266 tion of TCTA, which serves as an exciton-blocking layer
 267 owing to its high triplet energy ($E_T = 2.76$ eV),^{8c} resulted
 268 in the disappearance of the α -NPD fluorescence and a
 269 dramatic increase in the device efficiency (33 lm/W, 26 cd/
 270 A). Presumably, this is due to the fact that despite the
 271 recombination likely to occur on the TCTA-TPBI interface,

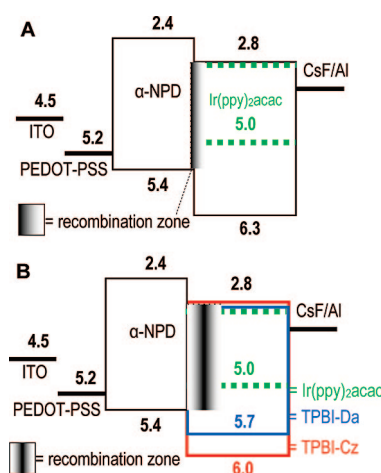


Figure 4. Energy level diagram of the PhOLEDs with TPBI (A) and TPBI-Cz and TPBI-Da (B). Plausible charge recombination-exciton generation zone is also shown. The HOMO-LUMO levels of TPBI are referenced to the values in the literature,^{16c} and those of new host materials are derived from the electrochemical (DPV) data and corrected using the TPBI levels known from the literature.^{16c}

272 all excitons are harvested by the TPBI-Ir(ppy)₂(acac) layer.
 273 Hence, the device efficiency was increased from 21 to 33
 274 lm/W, albeit at a cost of another layer.

275 As expected, the simple three-layer devices (Figure 3A),
 276 both TPBI-Cz and TPBI-Da based devices, did not display
 277 α -NPD fluorescence but show a dramatic increase in the
 278 efficiency, reaching the power efficiencies of 46 and 70 lm/W
 279 at a luminance of 10 cd/m² (Figure 5). The comparison of
 280 the external quantum efficiencies (EQE, %, at 0.1 mA/cm²)
 281 was also performed for the four devices (TPBI-only, TCTA-
 282 TPBI, TPBI-Cz, and TPBI-Da). Compared to the parent
 283 three-layer TPBI-only device, significant improvements in
 284 EQE were achieved in the devices with new hosts TPBI-Cz
 285 and TPBI-Da. Both the devices based on TPBI-Cz and TPBI-
 286 Da exhibited the maximum EQE in excess of 14%, whereas
 287 TPBI-only and TCTA-TPBI OLEDs displayed EQE of 4.7%
 288 and 5.7%, respectively. We presume that this is due to the
 289 formation of a more diffuse charge recombination zone
 290 located deeper in the doped TPBI-Cz/Da layer, as shown in
 291 Figure 4B. Such a diffuse zone would naturally display lower
 292 exciton density, thus decreasing the efficiency of undesirable
 293 effect such as triplet-triplet annihilation.⁵ These results seem
 294 to confirm our hypothesis that the bipolar transporter hosts
 295 would increase the efficiency of the devices using simple
 296 architectures.

297 While the devices with new host materials exhibited a
 298 higher efficiency, it is interesting to note that a lower driving
 299 voltage was observed in the TPBI and TPBI-Da devices
 300 compared to the TPBI-Cz one. A possible explanation is that
 301 the low HOMO level of TPBI also causes charge trapping
 302 by dopant molecules adjacent to the hole-injection layer
 303 (Figure 4). On the other hand, TPBI-Da has the highest
 304 HOMO level of the three hosts facilitating the hole injection
 305 into the emissive layer and therefore is likely to display a
 306 more balanced charge transport compared to TPBI-Cz.

307 Comparing the data in Table 2 with the literature results
 308 on green PhOLEDs, we realized that the current and power
 309 efficiencies of these devices are among the few best in the
 310 field. In comparison, Tokito et al. have reported a four-layer

(21) Goushi, K.; Kwong, R.; Brown, J. J.; Sasabe, H.; Adachi, C. *J. Appl. Phys.* **2004**, *9*, 5-7798.

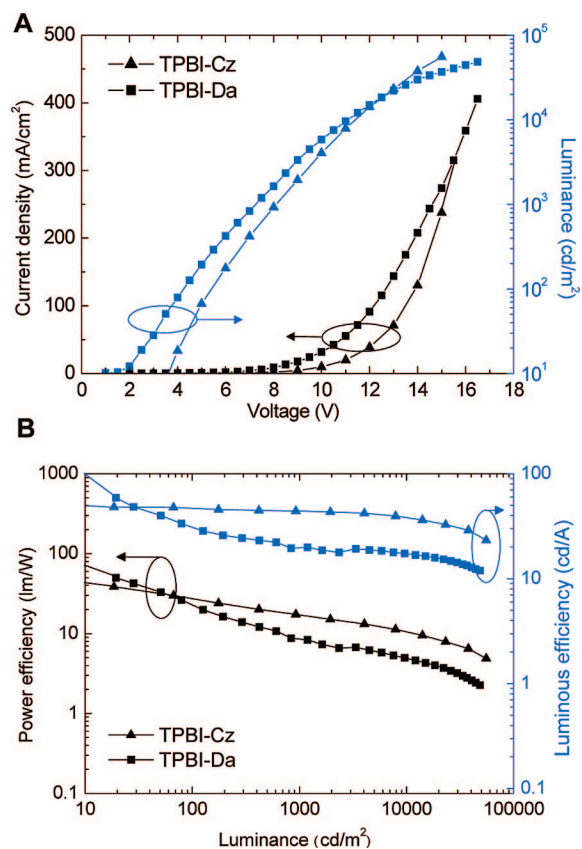


Figure 5. Panel A: Applied voltage–luminance characteristic of the devices. Panel B: Luminance–power efficiency and luminance–luminous efficiency characteristics of the devices. The corresponding graphs that include also the reference devices are in the Supporting Information.

311 device displaying power efficiency of 72 lm/W (64 cd/A)
 312 using the TCTA host and a new hole-exciton-blocking
 313 layer.^{9a} Similarly, other groups have recently reported the
 314 efficiencies of 64 lm/W^{16g} and approximately 48 lm/W^{16f} with
 315 the TCTA/TPBI codeposited mixed host and the extra hole-
 316 blocking, electron-transport layers. These device architectures
 317 are still complicated, and the power efficiencies are lower
 318 compared to the data obtained for TPBI-Cz/Da devices. In
 319 this study, we could achieve the maximum current efficien-
 320 cies of 48 and 60 cd/A (the power efficiencies of 46 and 70
 321 lm/W) from three-layer devices with TPBI-Cz and TPBI-
 322 Da host. This is one of the few PhOLEDs with less than
 323 four organic layers²² that show current efficiency exceeding
 324 55 cd/A while most of the two or three-layer devices show
 325 a lower efficiency.^{8h,16b,e,23} This suggests that the utilization
 326 of new TPBI-based bipolar hosts provides a great opportunity
 327 for fabrication of low-cost devices with reasonably high
 328 efficiency.

329 Conclusion

330 New bipolar host materials based on 1,3,5-tris(*N*-phenyl-
 331 benzimidazol-2-yl)benzene (TPBI) with attached carbazole
 332 and diphenylamine groups were designed and synthesized.

(22) (a) Ding, J.; Gao, J.; Cheng, Y.; Xie, Z.; Wang, L.; Ma, D.; Jing, X.; Wang, F. *Adv. Funct. Mater.* **2006**, *16*, 575. (b) Yang, X.; Müller, D. C.; Neher, D.; Meerholtz, K. *Adv. Mater.* **2006**, *18*, 948. (c) Haldi, A.; Domercq, B.; Kippelen, B.; Hreha, R. D.; Cho, J.-Y.; Marder, S. R. *Appl. Phys. Lett.* **2008**, *92*, 253502.

The DFT calculations suggested desirable distribution of
 HOMO and LUMO densities, suggesting potential for bipolar
 charge transport. The electrochemistry and UV–vis spec-
 troscopy was then used to estimate the actual HOMO and
 LUMO levels, which showed a good match with the data
 obtained from DFT calculations. Here, the electrochemical
 and phosphorescence studies revealed that neither the LUMO
 level nor the triplet energies differ significantly from the
 parent TPBI suggesting that the new materials would be
 suitable as hosts capable of both electron and hole transport
 and suitable for harvesting green electrophosphorescence.
 The green phosphorescent OLEDs with a simple three layer
 architecture using these new host materials achieved sig-
 nificantly better efficiency of 46 and 70 lm/W at a luminance
 of 10 cd/m² compared with devices using TPBI host as well
 as a more complex device utilizing TCTA exciton blocking
 layer. As a result of their high power efficiency and simple
 architectures, the new bipolar host materials might find
 applications in low-cost electroluminescent devices in solid-
 state lighting and large-area light sources. Future efforts will
 focus on further improvements in the charge-transport
 balance and application for blue-green phosphorescence,
 which in conjunction with an orange dopant may then be
 used for fabrication of low-cost white-light sources.²⁴

Experimental Section

Synthesis of TPBI-Br₃, TPBI-Cz, and TPBI-Da. *N*-(4-Bromophen-
 yl)-*N'*-(2-nitrophenyl)amine. A mixture of 1-fluoro-2-nitrobenzene
 (4.40 g, 31.7 mmol), 4-bromoaniline (10.9 g, 63.4 mmol), and
 potassium fluoride (2.30 g, 39.6 mmol) was heated at 170–180 °C
 for 72 h. The resulting mixture was dissolved in CH₂Cl₂ (500 mL)
 and washed with water (120 mL × 2) and brine (120 mL). Then,
 the CH₂Cl₂ solution was dried over Na₂SO₄. The filtrate was
 evaporated in vacuo to give a crude mixture, which was subjected
 to column chromatography on silica gel (solvent: CH₂Cl₂). The
 resulting red solid was recrystallized from EtOH to afford *N*-(4-
 bromophenyl)-*N'*-(2-nitrophenyl)amine as orange needles (5.7 g,
 61%). ¹H NMR (300 MHz, CDCl₃, δ): 9.39 (s, 1H), 8.21 (d, *J* =
 8.7 Hz, 1H), 7.53 (d, *J* = 8.7 Hz, 2H), 7.39 (t, *J* = 7.8 Hz, 1H),
 7.14–7.21 (m, 3H), 6.81 (t, *J* = 7.8 Hz, 1H). ¹³C APT NMR (75.5
 MHz, CDCl₃, δ): 142.4 (C), 138.0 (C), 135.8 (CH), 133.7 (C), 132.8
 (CH), 126.8 (CH), 125.7 (CH), 118.4 (C), 118.1 (CH), 116.0 (CH).
 EI-MS (*m/z*): 292 [M⁺]. Mp 161–163 °C.

N-(4-Bromophenyl)-1,2-phenylenediamine. A suspension of *N*-(4-
 bromophenyl)-*N'*-(2-nitrophenyl)amine (5.70 g, 19.4 mmol)
 and stannous chloride dihydrate (22.0 g, 97.0 mmol) in EtOH (250 mL)
 was refluxed for 24 h. After the reaction, the solvent was evaporated
 in vacuo. Then, water (500 mL) was added to the residue, followed
 by neutralization with NaHCO₃. The resulting solution was extracted
 with EtOAc (300 × 3 mL), and the combined organic layers were
 washed with water. The EtOAc solution was dried over Na₂SO₄,
 and the filtrate was evaporated in vacuo to obtain the product (4.1
 g, 80%). ¹H NMR (300 MHz, CDCl₃, δ): 7.28 (d, *J* = 9.0 Hz,

(23) (a) Lo, S.-C.; Male, N. A. H.; Markham, J. P. J.; Magennis, S. W.;
 Burn, P. L.; Salata, O. V.; Samuel, I. D. W. *Adv. Mater.* **2002**, *14*,
 975. (b) Bera, R. N.; Cumpstey, N.; Burn, P. L.; Samuel, I. D. W.
Adv. Funct. Mater. **2007**, *17*, 1149. (c) Wu, C.-H.; Shih, P.-I.; Shu,
 C.-F.; Chi, Y. *Appl. Phys. Lett.* **2008**, *92*, 233303. (d) Gao, Z. Q.; Mi,
 B. X.; Tam, H. L.; Cheah, K. W.; Chen, C. H.; Wong, M. S.; Lee,
 S. T.; Lee, C. S. *Adv. Mater.* **2008**, *20*, 774.
 (24) Anzenbacher, P., Jr.; Montes, V. A.; Takizawa, S. *Appl. Phys. Lett.*
2008, *93*, 163302.

385 2H), 7.01–7.10 (m, 2H), 6.73–6.82 (m, 2H), 6.60 (d, $J = 9.0$ Hz,
386 2H), 5.18 (s, 1H), 3.75 (s, 2H). ^{13}C APT NMR (75.5 MHz, CDCl_3 ,
387 δ): 144.9 (C), 142.5 (C), 132.4 (CH), 128.0 (C) 126.6 (CH), 125.6
388 (CH), 119.5 (CH), 117.0 (CH), 116.6 (CH), 111.3 (C). EI-MS (m/z):
389 262 [M^+]. Mp 118–122 °C.

390 1,3,5-Tris[*N*-(4-bromophenyl)benzimidazol-2-yl]benzene (TPBI-
391 Br₃). *N*-(4-bromophenyl)-1,2-phenylenediamine (1.64 g, 6.23 mmol)
392 was dissolved in 1-methyl-2-pyrrolidinone (NMP) (7 mL). To the
393 solution was added 1,3,5-benzenetricarbonyl trichloride (0.551 g,
394 2.08 mmol) portionwise under nitrogen. The reaction mixture was
395 stirred at room temperature for 2 h, and the reaction temperature
396 was then raised to 50 °C for an additional 30 min. After cooling,
397 the reaction mixture was poured into cold water (50 mL). The
398 resulting precipitates were filtered off and washed with water to
399 give crude tribenzamide. The tribenzamide was heated at 250 °C
400 for 3 h under nitrogen. After cooling, water (50 mL) was added to
401 the mixture and extracted with CH_2Cl_2 (50 \times 3 mL). The combined
402 organic layers were washed with water and brine, and then dried
403 over Na_2SO_4 . Solvent of the filtrate was removed in vacuo to obtain
404 a crude solid. 1,3,5-Tris[*N*-(4-bromophenyl)benzimidazol-2-yl]ben-
405 zene was isolated by silica gel column chromatography (solvent:
406 EtOAc) (1.63 g, 88%). ^1H NMR (300 MHz, CDCl_3 , δ): 7.87 (s,
407 3H), 7.85 (d, $J = 7.5$ Hz, 3H), 7.60 (d, $J = 8.7$ Hz, 6H), 7.27–7.39
408 (m, 6H), 7.18 (d, $J = 7.4$ Hz, 3H), 7.06 (d, $J = 8.7$ Hz, 6H). ^{13}C
409 APT NMR (75.5 MHz, CDCl_3 , δ): 150.6 (C), 143.2 (C), 137.3
410 (C), 135.8 (C), 133.6 (CH), 131.3 (CH), 131.1 (C), 129.1 (CH),
411 124.3 (CH), 123.8 (CH), 123.0 (C), 120.6 (CH), 110.6 (CH).
412 MALDI-TOF-MS (m/z): 893 [$\text{M} + \text{H}^+$]. Anal. Calcd for
413 $\text{C}_{45}\text{H}_{27}\text{Br}_3\text{N}_6$: C, 60.63; H, 3.05; N, 9.43. Found: C, 60.71; H, 2.93;
414 N, 9.47.

415 1,3,5-Tris[*N*-(4-carbazolylphenyl)benzimidazol-2-yl]benzene (TPBI-
416 Cz). A mixture of 1,3,5-tris[*N*-(4-bromophenyl)benzimidazol-2-
417 yl]benzene (0.800 g, 0.897 mmol), carbazole (0.900 g, 5.38 mmol),
418 CuI (0.049 g, 0.256 mmol), 18-crown-6 (0.093 g, 0.352 mmol),
419 and K_2CO_3 (1.10 g, 7.99 mmol) was heated in 1,3-dimethyl-3,4,5,6-
420 tetrahydro-2(1*H*)-pyrimidinone (DMPU) (2 mL) at 210 °C for 64 h
421 under nitrogen. After cooling, 1 N HCl (60 mL) was added to the
422 reaction mixture and extracted with CH_2Cl_2 (100 \times 3 mL). The
423 combined organic layers were washed with 15% NH_4OH (100 mL),
424 water (100 mL), and brine (100 mL). Then, the solution was dried
425 over Na_2SO_4 , and filtration followed by evaporation of solvent in
426 vacuo gave a brown oil. TPBI-Cz was isolated by silica gel column
427 chromatography (solvent: EtOAc/ $\text{CH}_2\text{Cl}_2 = 1/2$) (0.490 g, 44%).
428 ^1H NMR (300 MHz, CDCl_3 , δ): 8.13 (s, 3H), 8.06 (d, $J = 7.8$ Hz,
429 6H), 7.91 (d, $J = 7.8$ Hz, 3H), 7.60 (d, $J = 8.7$ Hz, 6H), 7.36–7.46
430 (m, 15H), 7.17 (t, $J = 7.4$ Hz, 6H), 7.07 (d, $J = 8.1$ Hz, 6H),
431 6.84–6.98 (m, 6H). ^{13}C APT NMR (75.5 MHz, CDCl_3 , δ): 150.5
432 (C), 143.3 (C), 140.7 (C), 138.3 (C), 137.1 (C), 135.5 (C), 131.4
433 (CH), 130.9 (C), 129.1 (CH), 129.0 (CH), 126.3 (CH), 124.3 (CH),
434 123.7 (CH), 123.6 (C), 120.8 (CH), 120.5 (CH), 120.5 (CH), 110.7
435 (CH), 109.3 (CH). MALDI-TOF-MS (m/z): 1150 [$\text{M} + \text{H}^+$]. Anal.
436 Calcd for $\text{C}_{81}\text{H}_{51}\text{N}_9$: C, 84.57; H, 4.47; N, 10.96. Found: C, 84.35;
437 H, 4.22; N, 11.13.

438 1,3,5-Tris[*N*-(4-diphenylaminophenyl)benzimidazol-2-yl]benzene (TPBI-
439 Da). A mixture of 1,3,5-tris[*N*-(4-bromophenyl)benzimidazol-2-
440 yl]benzene (0.500 g, 0.560 mmol), diphenylamine (0.570 g, 3.36
441 mmol), Pd(OAc)₂ (0.220 mmol), P(*t*-Bu)₃ (0.900 mmol), and
442 NaO*t*Bu (0.480 g, 4.99 mmol) in toluene (5 mL) was refluxed at

110 °C for 70 h under nitrogen. To the reaction mixture was added
443 water (50 mL), and extraction with CH_2Cl_2 (50 \times 3 mL) was
444 performed. The combined CH_2Cl_2 layers were washed with water
445 and dried over Na_2SO_4 . The solution was filtered, and the solvent
446 was removed in vacuo. The residue was subjected to column
447 chromatography on silica gel (solvent: EtOAc/ $\text{CH}_2\text{Cl}_2 = 1/2$
448 followed by 1/1) to afford TPBI-Da (0.598 g, 92%). ^1H NMR (300
449 MHz, CDCl_3 , δ): 7.89–7.91 (m, 6H), 7.33–7.42 (m, 9H),
450 6.87–7.00 (m, 42H). ^{13}C APT NMR (75.5 MHz, CDCl_3 , δ): 151.2
451 (C), 148.6 (C), 147.2 (C), 143.2 (C), 137.3 (C), 131.3 (CH), 130.7
452 (C), 129.9 (C), 129.5 (CH), 128.3 (CH), 124.9 (CH), 124.8 (CH),
453 123.8 (CH), 123.7 (CH), 123.2 (CH), 120.4 (CH), 110.8 (CH).
454 MALDI-TOF-MS (m/z): 1156 [$\text{M} + \text{H}^+$]; Anal. Calcd for $\text{C}_{81}\text{H}_{57}\text{N}_9$:
455 C, 84.13; H, 4.97; N, 10.90. Found: C, 83.76; H, 4.77; N, 10.84.
456 None of the three compounds, TPBI, TPBI-Cz, or TPBI-Da, show
457 clearly observable glass transition in the DSC measurement, while
458 showing sharp peaks corresponding to the melting point.

459 **Materials for OLED Fabrication.** Poly(3,4-ethylenedioxythio-
460 phene)/poly(styrene sulfonate) (PEPOT:PSS) was purchased from
461 H.C. Starck (Clevios P VP Al 4083). 4,4'-Bis[*N*-(1-naphthyl)-*N*-
462 phenylamino]biphenyl (α -NPD) as a hole-transporting layer and
463 4,4',4''-tris(*N*-carbazolyl)triphenylamine (TCTA) as an exciton
464 blocking layer were purchased from H.W. Sands Corporation and
465 Sigma-Aldrich, respectively. Iridium(III) bis(2-phenylpyridinato-
466 N, C^2)acetylacetonate [$\text{Ir}(\text{ppy})_2(\text{acac})$] was prepared according to
467 the literature method.²⁵ All the materials including TPBI and new
468 materials, except for PEDOT:PSS, were purified by train sublima-
469 tion prior to OLED fabrication.

470 **OLED Fabrication and Measurement.** OLEDs were fabricated
471 on glass-coated ITO substrates from Colorado Concept Coatings
472 (150–200 nm thick, $R_{\square} \sim 20 \Omega/\square$). The ITO-coated substrates
473 were degreased by detergent and organic solvents and then UV-
474 ozone cleaned to increase the ITO work function. PEDOT:PSS was
475 spin-coated over 1 \times 1 in. ITO substrates at 3000 rpm and baked
476 at 150 °C for 15 min. Organic layers were deposited at ~ 0.1 nm/s
477 in a high-vacuum chamber (10^{-7} torr, Angstrom Engineering). The
478 electron injection buffer layer CsF (1 nm) and aluminum cathode
479 (100 nm) were also deposited by thermal evaporation at ~ 0.02 nm/s
480 and 0.2 nm/s through a shadow mask. All the electrical and optical
481 characterization of the diodes was performed with an integration
482 sphere using C9920-12 External Quantum Efficiency Measurement
483 System (Hamamatsu Photonics) using a Keithley 2400 sourcemeter.
484 All the characterization of the devices was performed inside a
485 nitrogen-filled glovebox.
486

487 **Acknowledgment.** Financial support from AFOSR (FA9550-
488 05-1-0276 to P.A.), the State of Ohio (WCI-PVIC), and BGSU
489 is gratefully acknowledged.

490 **Supporting Information Available:** Phosphorescence spectra
491 of TPBI, TPBI-Cz, and TPBI-Da; figures for the device charac-
492 teristics. This material is available free of charge via the Internet
493 at <http://pubs.acs.org>.

CM9004954 494

(25) Lamansky, S.; Djurovich, P.; Murphy, D.; Abdel-Razzaq, F.; Kwong,
R.; Tsyba, I.; Bortz, M.; Mui, B.; Bau, R.; Thompson, M. E. *Inorg.*
Chem. **2001**, *40*, 1704.